Journal of Molecular and Cellular Cardiology 50 (2011) 863–871

Contents lists available at ScienceDirect

Journal of Molecular and Cellular Cardiology

journal homepage: www.elsevier.com/locate/yjmcc

Original article

Local control of β-adrenergic stimulation: Effects on ventricular myocyte electrophysiology and Ca^{2+}-transient☆

Jordi Heijman [a,b,c,1], Paul G.A. Volders [a], Ronald L. Westra [b], Yoram Rudy [c,*]

[a] Department of Cardiology, Cardiovascular Research Institute Maastricht, Maastricht University Medical Centre, P.O. Box 5800, 6202 AZ Maastricht, The Netherlands
[b] Department of Knowledge Engineering, Maastricht University, P.O. Box 616, 6200 MD Maastricht, The Netherlands
[c] Cardiac Bioelectricity and Arrhythmia Center, Washington University, Campus Box 1097, St. Louis, MO 63130-4899, USA

ARTICLE INFO

Article history:
Received 19 October 2010
Received in revised form 3 February 2011
Accepted 9 February 2011
Available online 21 February 2011

Keywords:
Computer modeling
Adrenergic stimulation
Cardiac electrophysiology
Compartmentalization

ABSTRACT

Local signaling domains and numerous interacting molecular pathways and substrates contribute to the whole-cell response of myocytes during β-adrenergic stimulation (βARS). We aimed to elucidate the quantitative contribution of substrates and their local signaling environments during βARS to the canine epicardial ventricular myocyte electrophysiology and calcium transient (CaT). We present a computational compartmental model of βARS and its electrophysiological effects. Novel aspects of the model include localized signaling domains, incorporation of β1 and β2 receptor isoforms, a detailed population-based approach to integrate the βAR and Ca^{2+}/Calmodulin kinase (CaMKII) signaling pathways and their effects on a wide range of substrates that affect whole-cell electrophysiology and CaT. The model identifies major roles for phosphodiesterases, adenylyl cyclases, PKA and restricted diffusion in the control of local cAMP levels and shows that activation of specific cAMP domains by different receptor isoforms allows for specific control of action potential and CaT properties. In addition, the model predicts increased CaMKII activity during βARS due to rate-dependent accumulation and increased Ca^{2+} cycling. CaMKII inhibition, reduced compartmentation, and selective blockade of β1AR is predicted to reduce the occurrence of delayed afterdepolarizations during βARS. Finally, the relative contribution of each PKA substrate to whole-cell electrophysiology is quantified by comparing simulations with and without phosphorylation of each target. In conclusion, this model enhances our understanding of localized βAR signaling and its whole-cell effects in ventricular myocytes by incorporating receptor isoforms, multiple pathways and a detailed representation of multiple-target phosphorylation; it provides a basis for further studies of βARS under pathological conditions.

1. Introduction

Maximal β-adrenergic receptor (βAR) stimulation (βARS) in ventricular myocytes activates the βAR/G-protein/adenylyl cyclase (AC)/cyclic AMP (cAMP)/protein kinase A (PKA) pathway that results in the phosphorylation of numerous intracellular proteins ("substrates") including the L-type Ca^{2+} channel ($I_{Ca,L}$), slowly activating delayed rectifier K^+ channel (I_{Ks}), phospholamban (PLB) and the inhibitory troponin subunit (TnI). In addition, there are several feedback loops, such as βAR desensitization, that control the temporal response of βARS [1,2]. Observations in living myocytes using fluorescent techniques have demonstrated the importance of localized signaling domains in βAR cascade function. Moreover, many interdependencies were identified between PKA substrates that influence the cardiac action potential (AP) and calcium transient (CaT) [3,4].

Localized signaling results from physical subcellular domains with restricted diffusion of the second messenger cAMP (e.g., caveolae), from specific subcellular localization of signaling molecules (e.g., cAMP and phosphodiesterases; PDEs) and from targeting of PKA to specific substrates by A-kinase anchoring proteins (AKAPs) [5–7]. Localized signaling in subcellular domains is essential for precise specific regulation ("local control"); it allows multiple signaling cascades that affect cAMP to target specific substrates. This local organization may change in pathologies such as heart failure [8]. The relative contribution of each local signaling domain and substrate to the whole-cell electrophysiological response during βARS is extremely difficult to determine experimentally, especially in large mammals. Moreover, an increasing number of interactions between the βAR signaling cascade and other signaling cascades, most prominently the Ca^{2+}/Calmodulin kinase (CaMKII), are discovered to play an important role in normal physiology and in pathology [9]. Currently, our understanding of the complex interactions between signaling

☆ Abbreviations are defined in the online data supplement.

* Corresponding author. Tel.: +1 314 935 8160; fax: +1 314 935 8168.
E-mail addresses: jordi.heijman@maastrichtuniversity.nl (J. Heijman), rudy@wustl.edu (Y. Rudy).
[1] Tel.: +1 314 935 8160; fax: +1 314 935 8168.

0022-2828/$ – see front matter © 2011 Elsevier Ltd. All rights reserved.
doi:10.1016/j.yjmcc.2011.02.007

cascades and substrates and their effects on cellular electrophysiology is rather limited.

Computational approaches have been employed to enhance our understanding of various (patho)physiological processes [10]. The computational approach is particularly useful when the system under investigation is complex, highly interactive and nonlinear, as is the case with the βAR cascade and its effects on cellular electrophysiology. Quantitative studies of cAMP signaling have been performed [11–13] but did not include electrophysiological effects. Several studies have modeled different aspects of the adrenergic system in the ventricular myocyte in various levels of detail [14–18]. However, none of these studies described the effects of localized signaling domains or included all interacting PKA substrates. Here, we present the first detailed computational model of βARS in the canine ventricular myocyte that includes both localized signaling domains and a wide range of electrophysiological substrates. We use this model to study the local effects of βARS on subcellular targets and their consequences in terms of whole-cell electrophysiology and CaT.

2. Methods

Details of the computational model (Fig. 1) are provided in the online data supplement. Key features are highlighted subsequently.

2.1. βAR signaling cascade

A recent compartmental model of cAMP signaling in ventricular myocytes served as a starting point for the βAR-signaling model of this study [11]. Three functional compartments represent the caveolar (CAV), extracaveolar membrane (ECAV) and cytosolic (CYT) signaling domains. Each compartment contains signaling proteins at local concentrations. We extend the cAMP signaling cascade with

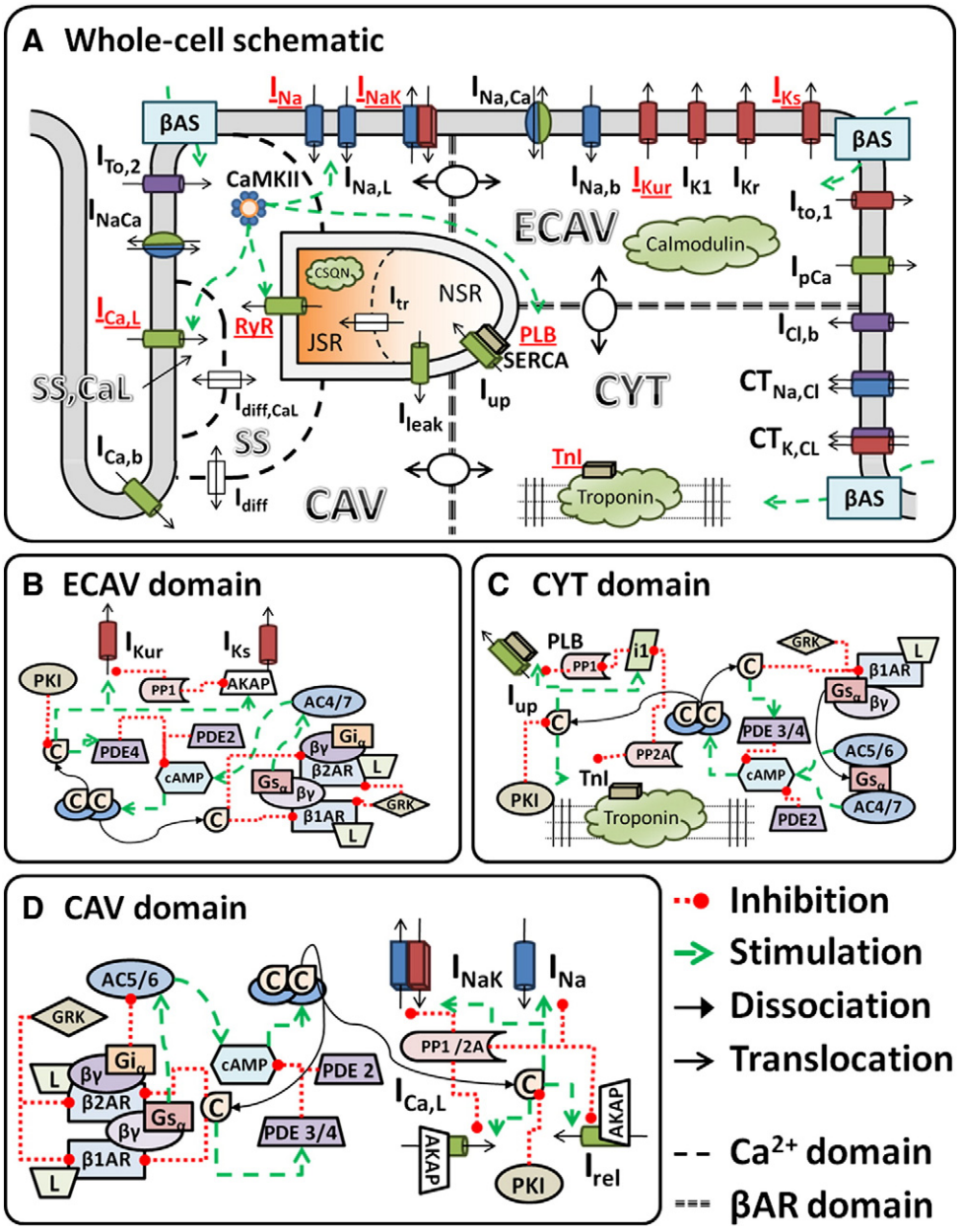

Fig. 1. A. Schematic of the canine ventricular cell model including Ca^{2+} handling, electrophysiology, CaMKII signaling pathway and βAR signaling domains. Substrates modulated by PKA phosphorylation are indicated in red. Model CaMKII targets include PLB/Serca and RyR. B–D, Detailed schematics of the interactions in the extracaveolar (ECAV; B), cytosolic (CYT; C) and caveolar (CAV; D) signaling domains. Abbreviations are defined in the section 1.1 of the online data supplement. Model code is provided in the Research Section of http://www.rudylab.wustl.edu.

differential localization of β_1AR and β_2AR, local PKA activation (high affinity PKAI in CYT, lower affinity PKAII in CAV and ECAV), PKA-dependent feedback loops, PKA targeting to I_{CaL}, I_{Ks} and RyR by AKAPS, and eight substrates of direct PKA-dependent phosphorylation. Figs. 1 B–D show the schematics of the compartmental signaling cascades in the model. Substrates were placed in CAV (I_{CaL} I_{Na}, I_{NaK}, and RyR) based on their association with caveolin-3. Other sarcolemmal substrates (I_{Ks} and I_{Kur}) were placed in ECAV. The remaining substrates (PLB and TnI) were located in CYT.

All biochemical reactions were modeled either as differential equations (e.g., cAMP production, PKA activation, and receptor desensitization) or as algebraic equations based on steady-state assumptions for reactions occurring much faster than changes in cAMP and substrate phosphorylation. Time-dependent concentrations of the βAR agonist isoproterenol (ISO, in combination with blockade of either β_1AR or β_2AR in some simulations) and/or the PDE inhibitor IBMX served as inputs to the adrenergic signaling cascade.

2.2. Analysis of cAMP compartmentation

Experimentally, compartmentation of cAMP is revealed by differential effects of signaling pathways that affect cAMP on phosphorylation of cytosolic versus sarcolemmal proteins [5,19], and by differences in cytosolic cAMP and subsarcolemmal cAMP levels measured with fluorescent probes and cyclic nucleotide-gated channels [20], respectively. This has illustrated that selective augmentation of cAMP in specific compartments occurs and is critical for specific regulation of subcellular targets. Here, we focus on the effects of βARS. Other signaling pathways affecting cAMP (e.g., the prostaglandin receptor PGE1) are not included. Compartmentation has also been shown through differences in βAR isoform stimulation. In mammalian ventricle, three isoforms have been reported. In canine, approximately 80% are β_1AR [21]. Functional effects of β_2AR stimulation are highly dependent on species and experimental conditions. In rodents, β_2ARS only affects local cAMP concentrations, whereas cAMP increases elicited by β_1ARS diffuse throughout the cell [22,23]. Studies in the failing canine ventricle show a reduction in β_1AR without changes in β_2AR and consequently an important role of β_2ARS [24]. Under normal physiological conditions, differential effects of β_2ARS on whole-cell behavior have been reported [24–26]. The model includes β_1AR and β_2AR with cell-wide and CAV localization respectively, based on experimental data [8]. The functional significance of β_3AR in large mammals is incompletely understood and not included here [27]. Virtual knock-out models of selected signaling proteins were created by setting their concentration to 0. Reduced compartmentation was simulated by increasing the cAMP diffusion rates by a factor 1000.

2.3. CaMKII signaling cascade

The baseline model [28] includes phosphorylation of PLB and RyR by CaMKII. We included populations for CaMKII-dependent phosphorylation of I_{CaL}, I_{Na} and late I_{Na} ($I_{Na,L}$) based on recently published formulations [29], as well as CaMKII-dependent changes in I_{To} and I_{K1} (online supplement). CaMKII is activated by localized Ca^{2+} in the Ca^{2+} subspace, consistent with previous modeling studies, but no further localization is included. Additional crosstalk between βARS and CaMKII occurs via PKA-dependent activation of Inhibitor 1 and subsequent deactivation of PP1 that controls CaMKII deactivation, consistent with experimental observations [9].

2.4. Changes to electrophysiological substrates after phosphorylation

Phosphorylation effects were incorporated by including populations of phosphorylated and non-phosphorylated channels with distinct properties for the eight substrates affected by βARS. Properties of non-phosphorylated (baseline) substrates were based on the recently published model of the canine epicardial ventricular myocyte [28] and properties of phosphorylated channels were determined from experimental data in the presence of a saturating dose of ISO. At each time instant, the current/flux for a given substrate is determined for both (phosphorylated and non-phosphorylated) populations. The fraction of phosphorylated channels, which is determined by the βAR cascade, is then used to interpolate between these values to determine the net current/flux. We assume that phosphorylation by PKA and CaMKII is independent and have integrated the βAR and CaMKII cascades using four populations for these targets.

The population-based approach is based on the assumption that phosphorylation is a binary process that is independent of channel gating. It captures the distinct conformations of phosphorylated and non-phosphorylated channels as they coexist in the ventricular myocyte. Most previous modeling approaches employed only one homogeneous population and shifted model parameters (such as the $V_{1/2}$ of activation) based on phosphorylation levels [14,17]. Although both approaches coincide at phosphorylation levels of 0% and 100%, they are different for other levels (Supplemental Fig. S21).

2.5. Validation

The model is validated (Supplemental Figs. S1–S20) with a wide range of experimental data at the levels of the signaling cascade, individual electrophysiological components and whole-cell response.

3. Results

3.1. Whole-cell effects of βARS on APD and CaT

Subcellular alterations of various substrates in response to βARS combine at the cellular level to change the AP morphology and CaT. Fig. 2A shows that βARS results in shortening of APD and increase in AP plateau amplitude, consistent with experimental data [30]. Experimentally, there is considerable cell-to-cell variation in the magnitude of the response (Supplemental Fig. S22) and model output is within this range. At cycle length (CL) = 1000 ms, CaT amplitude is significantly enhanced and CaT decay is faster, as observed experimentally (Fig. 2B; Supplemental Fig. S19). We analyzed the rate-dependence of these APD and CaT changes by pacing the model to steady-state in absence or presence of a saturating dose of ISO at various CL. APD shortening and increased CaT amplitude are observed at all CL (Fig. 2C,D). Changes in CaT amplitude and Ca^{2+} loading are most pronounced at fast rates.

3.2. Contribution of individual PKA substrates to whole-cell AP and CaT changes in response to βARS

The relative contribution of a substrate was analyzed by pacing the model to steady-state in the absence of βARS, in the presence of 1.0 μmol/L ISO and with 1.0 μmol/L ISO but with the phosphorylation of the substrate of interest disabled. Fig. 3 summarizes the effects of phosphorylation of each substrate on APD (Fig. 3A), CaT amplitude (Fig. 3B) and CaT rate of decay (Fig. 3C) at CL = 350 ms (left) and CL = 2000 ms (right). AP and CaT traces underlying this data can be found in Supplemental Figs. S23 and S24.

I_{Ks} has only a small impact on steady-state APD under baseline conditions [28] but plays a major role in APD shortening during βARS, consistent with experimental observations [30]. Previous studies have identified kinetic channel states (termed available reserve) that modulate the rate-dependent contribution of I_{Ks} to repolarization [31,32] and their alteration by βARS [33,34]. Consistent with these studies, the model predicts an increased available reserve during βARS in the canine ventricular myocyte (Supplemental Fig. S25). Consistent with simpler models [16] and experimental evidence

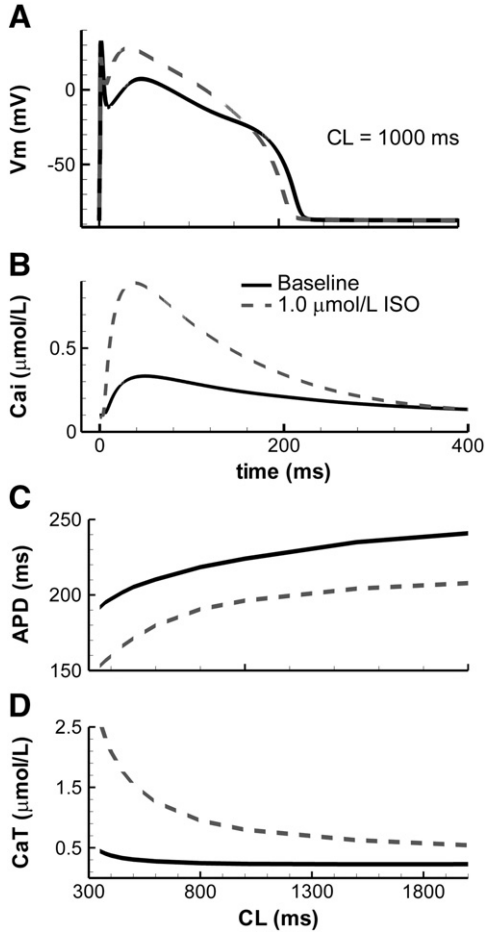

Fig. 2. Effect of βARS on whole-cell AP and CaT. Baseline shown in solid lines, maximal βARS in dashed lines. A. Steady-state AP at CL = 1000. B. Simulated calcium transient at CL = 1000 ms in the presence of βARS shows increased amplitude and rate of relaxation compared to baseline. C. Steady-state APD as a function of pacing CL. D. Steady-state CaT amplitude rate-dependence.

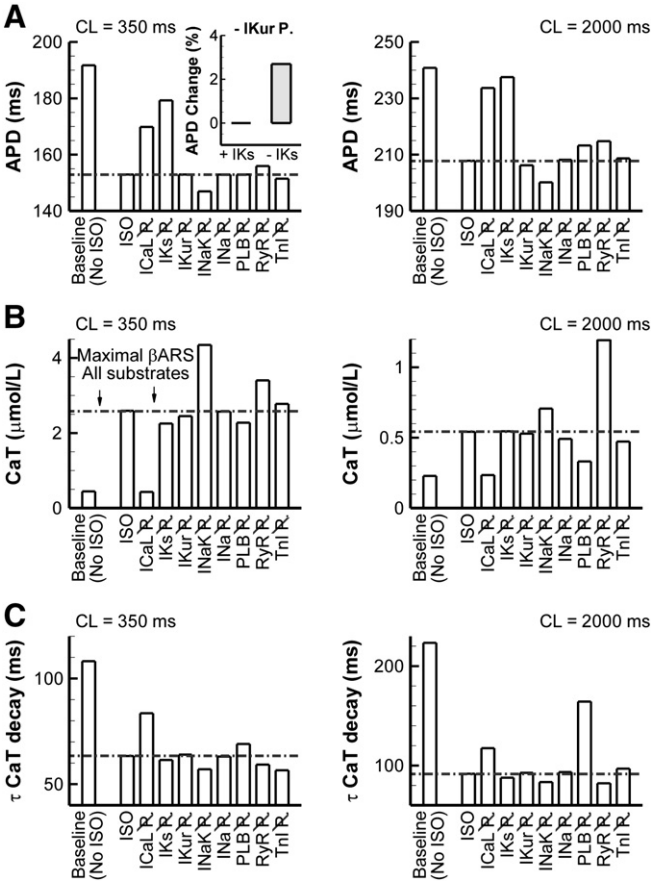

Fig. 3. Summary of contributions of individual substrates to APD and CaT changes in the presence of ISO (complete data are provided in Supplemental Figs. S23 and S24). A. Steady-state APD at CL = 350 ms (left) and CL = 2000 ms (right) at baseline (no ISO), in the presence of maximal βARS and during maximal βARS when PKA-dependent phosphorylation of a specific substrate is disabled (e.g., indicated by ICaL P for inhibition of I_{CaL} phosphorylation). CaMKII phosphorylation remained intact. The horizontal dashed-dotted line indicates the reference value during maximal βARS with all substrates phosphorylated. Inset shows the % increase in APD when I_{Kur} phosphorylation is disabled (versus when it is present) in the presence or absence of I_{Ks}. B. Similar to (A) for CaT amplitude. C. Similar to (A) for the time-constant of CaT decay based on a monoexponential fit.

[33,35], the model predicts a major role for I_{CaL} in the increased AP plateau potentials and increased inotropy observed during βARS. PLB phosphorylation is primarily responsible for the increased rate of CaT decay, particularly at slow rates. At fast rates, CaMKII phosphorylation (which is not inhibited in Fig. 3) reduces the impact of PKA-dependent phosphorylation. βARS increases Ca^{2+} leak from the SR [36]. Consistent with this observation, disabling RyR phosphorylation increases CaT, particularly at long CL.

The model provides new insights into the contribution of other substrates. Fig. 3B indicates that phosphorylation of I_{NaK} (through the accessory protein phospholemman) reduces cardiac inotropy (i.e., inhibition of I_{NaK} phosphorylation increases CaT amplitude). This was previously shown in mouse ventricular myocytes by Despa et al. [37] and we show that similar mechanisms apply in the dog, despite significant differences in Ca^{2+} handling between these species. The increase in CaT results from increased steady-state intracellular Na^+ levels that reduce Ca^{2+} extrusion via Na^+–Ca^{2+} exchange. Similar Na^+ accumulation resulting from βARS in the absence of I_{NaK} phosphorylation was previously shown in a model of the guinea-pig ventricular myocyte, although CaT amplitude was not quantified [17]. Interestingly, despite a reduction in repolarizing I_{NaK} when phosphorylation is inhibited, the increased CaT is accompanied by a shortening of APD (Fig. 3A). This occurs via reduced forward mode I_{NaCa} and enhanced Ca^{2+}-dependent inactivation of I_{CaL}. When Ca^{2+}-dependent inactivation was disabled for the final beat after pacing to steady state, APD shortening in the absence of I_{NaK} phosphorylation was reduced from 7.7 ms to 2.4 ms (Supplemental Fig. S27). Similarly, inhibition of I_{NaCa} reduced APD shortening to 2.5 ms.

Inhibition of I_{Kur} was recently predicted to have a significant APD-prolonging effect in canine ventricular myocytes [38] and, as such, augmentation of I_{Kur} by phosphorylation is expected to result in APD shortening. Interestingly, we do not find any effect on APD and only a modest effect on AP plateau amplitude when comparing normal βARS to βARS in the absence of I_{Kur} phosphorylation (Fig. 3A, Supplemental Fig. S23). However, in the absence of I_{Ks}, inhibition of I_{Kur} phosphorylation results in a significant additional prolongation of APD (2.7% increase compared to I_{Ks} block alone versus <0.1% increase in the presence of I_{Ks}, Fig. 3A, inset), as expected based on the dependence of APD prolongation on initial APD [39]. As such, I_{Kur} phosphorylation may still have important effects in pathological conditions and provide "repolarization reserve" when I_{Ks} is compromised by disease or drugs.

3.3. Localized cAMP signaling

Experimentally, it is established that cAMP levels are localized in subdomains. The control model with normal compartmentation shows distinct cAMP concentrations in CAV, ECAV and CYT domains at baseline, as well as in response to βARS (Fig. 4A; top-left panel). The

relative distribution of cAMP at baseline (micromolar range for ECAV, high nanomolar range for CAV and CYT) is consistent with that reported by Iancu et al. [11]. Activation of different signaling pathways can elicit specific subcellular cAMP responses. For example, β_2AR are predominantly located in caveolae [8] and simulated β_2ARS elevates CAV cAMP with only modest effects on cAMP in ECAV and CYT domains (Fig. 4A; bottom-left panel). In contrast, when cAMP diffusion barriers are reduced (e.g., simulating application of MβC, a cholesterol depleting agent that, among other things, disrupts local cAMP domains), cAMP concentrations become uniform throughout the cell and βARS results in cell-wide increase in cAMP independent of the activated receptor isoform, consistent with experiment [8] (Fig. 4A; right panels). In the control (compartmental) model (left panels), in contrast to APD *shortening* with whole-cell βARS, selective stimulation of β_2AR *prolongs* APD (Fig. 4B; top-left panel). However, increases in CaT are present for both types of βARS (bottom-left panel). When compartmentation is reduced (right), the subsarcolemmal cAMP levels in CAV and ECAV are too small to allow regulation of APD or CaT, which show a similar time-dependent change, independent of the receptor isoform that is stimulated (Fig. 4B; right panels). The mechanism underlying the distinct responses to whole-cell ($\beta_1+\beta_2$) βARS and β_2ARS-only in the compartmental model is shown in Fig. 4C. Whole-cell βARS phosphorylates substrates throughout the cell, including I_{Ks}, which is responsible for APD shortening (Fig. 3). In contrast, β_2ARS does not phosphorylate I_{Ks} or PLB (Fig. 4C; left panel). When compartmentation is reduced, the differential control of phosphorylation by the two isoforms is lost (Fig. 4C; right panel). Since MβC application alters the distribution of other signaling molecules in addition to cAMP diffusion, it is difficult to relate the predicted functional responses to experimental measurements in the presence of MβC [23].

To identify the main signaling components involved in establishing local cAMP levels, virtual knock-outs of these components were simulated in the absence and presence of βARS (Fig. 5). Specific subcellular distributions of PDEs, ACs and PKA cause inter-domain differences in local cAMP concentrations. In the absence of βARS, PDE3 (and to a lesser extent PDE4) and AC5/6 predominantly determine cAMP in CYT and CAV, while AC4/7 determines cAMP in ECAV. As expected, cAMP levels increase in all compartments upon βARS in control conditions and in all virtual knock-outs. In general, the localized differences occurring in knock-outs remain present during βARS (Fig. 5B). Several negative feedback loops exist in the βAR signaling cascade. In these loops PKA activated by cAMP modifies upstream elements in the cascade to limit excessive cAMP production. The model predicts that PKA-dependent feedback loops have important effects on steady-state cAMP levels and that this occurs in a localized manner (right-most bar graphs). There is a prominent increase in cAMP in the absence of PKA during βARS (Fig. 5B; far-right). This increase occurs via several feedback loops (Fig. 5C). Without PKA there is increased availability of βAR (Fig. 5C; left panel), due to reduced βAR desensitization. Moreover, there is reduction in cAMP hydrolyzing activity of PDE3 and PDE4 (Fig. 5C; middle panel). PDE3 and PDE4 can be phosphorylated by PKA, thereby increasing their activity. In the PKA knock-out model this negative-feedback on cAMP is removed, resulting in increased cAMP levels. Finally, there is no activation of Gi (due to

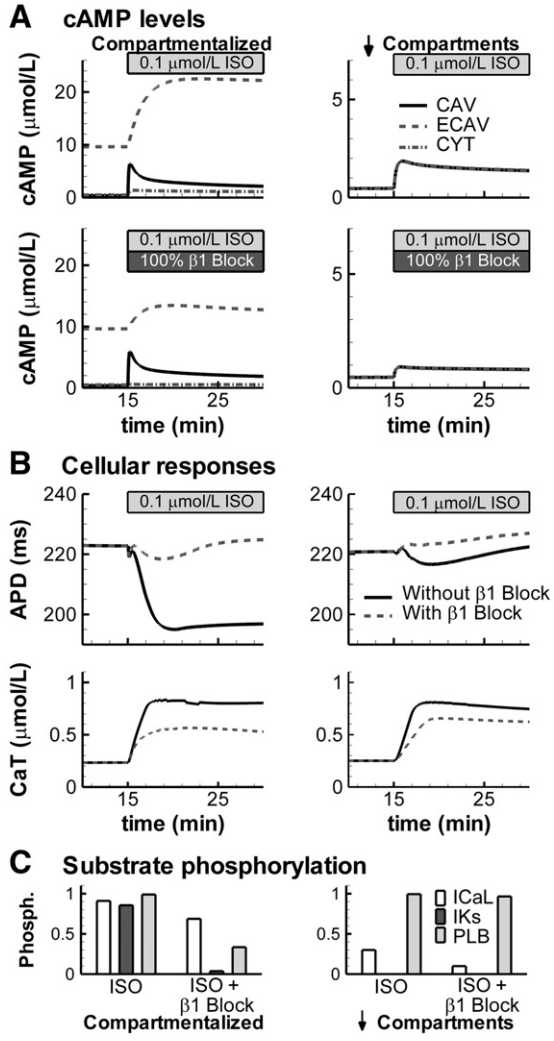

Fig. 4. Compartmentation of βARS in the control model with normal compartments (left) or in simulations with reduced compartmentation (right). A. Time dependent changes in cAMP levels in CAV (solid line), ECAV (dashed) and CYT (dash-dotted) during stimulation with 100 nmol/L ISO (top) or in the presence of β_2AR stimulation only (100 nmol/L ISO and 100% block of β_1AR; bottom). B. Differential effects of combined (β_1AR + β_2AR) stimulation (solid) or β_2ARS only (dashed) on APD (top) and CaT amplitude (bottom) at a cycle length of 1000 ms. C. Steady-state I_{CaL}, I_{Ks} and PLB phosphorylation levels during the simulations in (B).

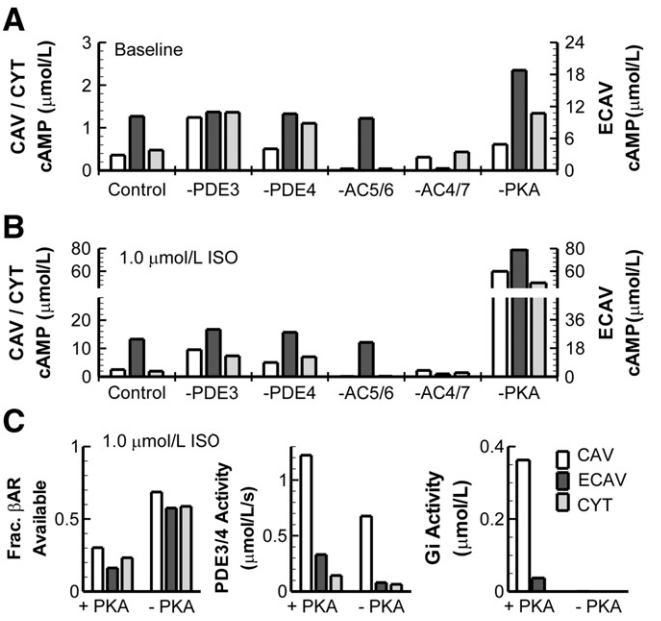

Fig. 5. Contribution of βAR signaling components to cAMP compartmentation. A. Effect of virtual knock-outs of PDE3, PDE4, AC5/6, AC4/7 or PKA on steady-state cAMP concentration in CAV, ECAV and CYT domains in the absence of βARS. B. Identical to A, in the presence of 1.0 μmol/L ISO. Note separate y-scale for cAMP in ECAV and different y-scales in (A) and (B). C. Mechanisms behind prominent cAMP increase resulting from virtual PKA knock-out in the presence of βARS. Difference in βAR availability (left), PDE3/4 Activity (at 1.0 μmol/L cAMP; middle) or Gi activity (right) in the presence and absence of PKA during stimulation with 1.0 μmol/L ISO for each compartment.

β2AR phosphorylation) in the absence of PKA, reducing inhibition of AC5/6.

3.4. Downstream effects of βARS on CaMKII

In addition to cAMP compartmentation, Ca^{2+} signaling is also highly localized. High subsarcolemmal Ca^{2+} concentrations in dyadic clefts (Ca^{2+}_{SS}) activate the CaMKII signaling pathway which phosphorylates several substrates that are also targeted by PKA. CaMKII activity in the model is rate-dependent, consistent with experimental observations [40,41]. ISO increases CaMKII activity in a concentration-dependent manner, particularly at fast rates (Fig. 6A). Increased CaMKII is caused by a larger peak Ca^{2+}_{ss} transient and a larger duration with Ca^{2+}_{ss} levels close to CaMKII affinity (Fig. 6B). In addition, there is an important role for reduction in PP1 via PKA-dependent activation of Inh1, since virtual knock-out of Inh1 significantly reduces CaMKII activity during maximal βARS (Fig. 6A; dash-double-dotted line), consistent with the effect of PP1 inhibition by okadaic acid in rat ventricular myocytes [42]. The rate-dependent increase in CaMKII is more pronounced than the increase due to enhanced Ca^{2+} cycling with βARS (e.g., CaMKII activity at CL = 350 ms without βARS is 0.15, compared to 0.06 at CL = 1500 ms with βARS). Therefore, the slow rate of CaMKII deactivation (time constant of deactivation is approximately 1500 ms [40]), which results in accumulation of active CaMKII at fast rates (Fig. 6C), has a larger impact on steady-state CaMKII activity than enhanced activation due to βARS-dependent increases in Ca^{2+} cycling. PLB is phosphorylated by PKA on Ser16 and by CaMKII on Thr17. Hagemann et al. analyzed the rate- and adrenergic-stimulation dependent modulation of PLB phosphorylation in rat ventricular myocytes [43]. The simulation results in Fig. 6D show an important role of pacing rate for CaMKII-dependent phosphorylation of PLB, whereas PKA-dependent phosphorylation is rate-independent, in agreement with Hagemann's experimental observations. Knock-out of Inh1 increases PP1 activity and reduces both Ser16 and Thr17 PLB phosphorylation.

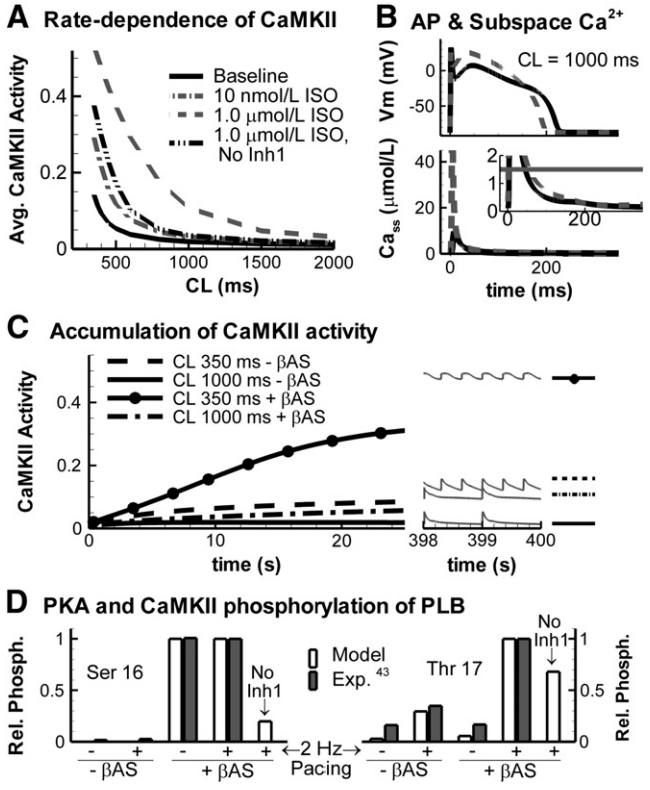

Fig. 6. A. Rate-dependence of steady-state CaMKII activity averaged per beat at baseline (solid black) and in the presence of 10 nmol/L ISO (dash-dotted, grey), 1.0 μmol/L ISO (dashed, grey) or 1.0 μmol/L ISO with virtual knock-out of Inh1 (dash-double dot, black). B. Steady-state AP and subsarcolemmal Ca^{2+} transient in the dyadic cleft at baseline (solid black) and during maximal βARS (dashed grey) at CL = 1000 ms. Horizontal line in magnified inset indicates the half maximal Ca^{2+} level for CaMKII activation. C. Accumulation of CaMKII activity during the first 25 seconds of pacing in the absence and presence of βARS at CL = 350 ms and CL = 1000 ms. Black lines indicate the average CaMKII per beat. Right part shows corresponding steady state unaveraged CaMKII traces. D. Phosphorylation of PLB by PKA at Ser 16 (left) and CaMKII at Thr 17 (right) at rest and during pacing in the absence or presence of adrenergic stimulation in the model (white bars) and in rat ventricular myocytes [43] (shaded bars).

3.5. Calcium overload and delayed afterdepolarizations

For the final set of simulations, the model was extended with a formulation for store-overload induced SR Ca^{2+} release. After cessation of pacing at CL = 500 ms in the presence of 1.0 μmol/L ISO, the model shows four Ca^{2+} after-transients and corresponding delayed afterdepolarizations (DADs; Fig. 7A). DAD characteristics are consistent with those measured in canine ventricular myocytes [44] (Fig. 7B). The effects of βAR isoforms, compartmental signaling and CaMKII on DADs are shown in Fig. 7C for various pacing CLs. At faster CL, Ca^{2+} load increases, more DADs are generated, their average amplitude increases (Fig. 7C) and coupling interval decreases (not shown). Inhibition of β1AR and, to a lesser extent, reduced compartmentation (via increased cAMP diffusion) reduce the number of DADs, in line with the lower CaT amplitudes observed in Fig. 4, although DADs were still observed at the fastest rates. Virtual knock-out of CaMKII, on the other hand, prevented DADs even at the fastest rate (3 Hz) investigated. Although all conditions reduce the incidence of DADs, this occurs via different mechanisms. β1AR blockade predominantly affects PKA-dependent phosphorylation of PLB, reduced compartmentation modestly reduces PKA-dependent phosphorylation of I_{CaL} and RyR, and CaMKII inhibition abolishes CaMKII-dependent phosphorylation of all substrates without altering the PKA-dependent phosphorylation (Fig. 7D). β1AR block or CaMKII inhibition strongly reduce the maximum JSR Ca^{2+} levels (Fig. 7E). This reduction in JSR Ca^{2+} explains the low incidence of DADs in these conditions since the threshold for spontaneous release is reached less often. To investigate which substrate has the largest impact on JSR Ca^{2+} levels and the incidence of DADs, we selectively inhibited either the PKA- or CaMKII-dependent phosphorylation of these 3 targets individually. The model predicts that PKA-dependent phosphorylation of I_{CaL} (in line with the strong reduction in CaT amplitude shown in Fig. 3), and both PKA- and CaMKII-dependent modulation of SR Ca^{2+} uptake (via SERCA2a and PLB phosphorylation) have the largest impact (not shown). Consistent with previous modeling studies [45], when an effect of RyR phosphorylation (by CaMKII and/or PKA) to lower the threshold for spontaneous Ca^{2+} release is included, this target also has a significant impact, enhancing DAD incidence (not shown). However, the functional consequences of RyR phosphorylation by both kinases are still actively debated in the literature [46].

4. Discussion

This study investigates the interplay between compartmentalization of the β-adrenergic signaling cascade and the different isoforms of the βAR in determining responses of whole-cell electrophysiology and calcium transient to βARS. The main novel mechanistic insights include: (i) compartmentation of cAMP is mainly controlled by PDEs, AC and PKA and allows for selective effects of β_1ARS and β_2ARS (see later discussion); (ii) I_{NaK} modulation by phospholemman phosphorylation alters $[Na^+]_i$ and consequently $[Ca^{2+}]_i$ to limit inotropy in large mammals; this alters APD via I_{NaCa} and Ca^{2+}-dependent inactivation of I_{CaL}; (iii) I_{Kur} phosphorylation enhances repolarization reserve when I_{Ks} is reduced, but does not affect APD for control I_{Ks};

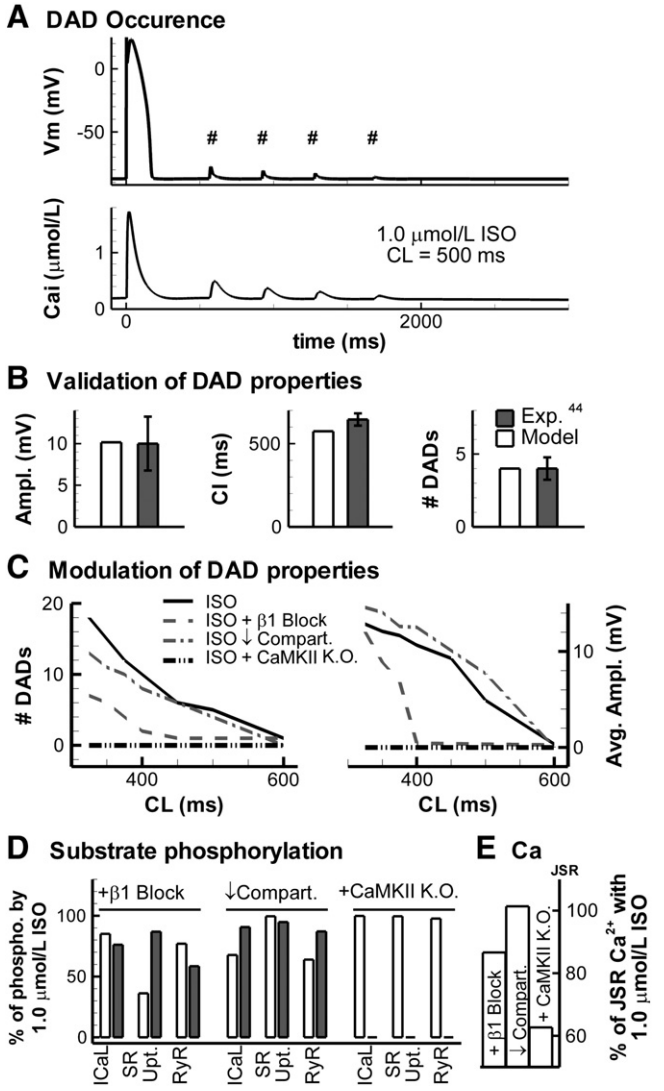

Fig. 7. A. DADs (top, indicated with #) and Ca^{2+} after-transients (bottom) after cessation of pacing (CL = 500 ms; last paced beat shown) in the presence of 1.0 μmol/L ISO. B. Comparison of DAD properties from A to experimental data from canine ventricular myocytes. DAD amplitude (left), DAD coupling interval (middle) and number of DADs (right). C. Modulation of number of DADs (left) and DAD amplitude (right) at different CLs by 1.0 μmol/L ISO (solid line), ISO + β1AR blockade (dashed), ISO with reduced compartmentation (dash-dotted), or ISO + CaMKII inhibition (dash-double dot). D. Phosphorylation of I_{CaL}, SERCa2a & PLB ("SR Upt."), and RyR by PKA (white bars) or CaMKII (shaded bars) relative to 1.0 μmol/L ISO at CL = 500 ms, for the conditions in C. E. Maximum JSR Ca^{2+} levels during β1AR blockade, reduced compartmentation, or CaMKII inhibition, relative to 1.0 μmol/L ISO at CL = 500 ms. K.O. = knock out.

(iv) inhibition of CaMKII, blockade of β_1AR and reduced compartmentation reduce the incidence of DADs during βARS at fast rates.

Substrates experience local signaling environments depending on their subcellular localization. The model identifies restricted diffusion and localized expression of PDEs, AC and PKA as the main elements controling cAMP compartmentation. Knock-out of PKA has a particularly strong effect on cAMP during βARS via disruption of 3 different negative-feedback loops (βAR desensitization, PDE stimulation and Gi activation via β2AR phosphorylation). Increased cAMP after PKA inhibition was also reported by Rochais et al. in rat ventricular myocytes [47], although their increase is less pronounced. Differences between specific PKA knock-out and (possibly incomplete) PKA inhibition with H89 may explain this difference. Interestingly, H89 has also been shown to block βAR in human airway cells [48], which would disable the disruption of one of the negative feedback loops.

Activation of specific cAMP domains by localized G-protein-coupled receptors can modulate whole-cell responses such as APD and CaT selectively. For example, activation of β_2AR alone does not phosphorylate I_{Ks} or PLB and prolongs APD, but has a modest positive inotropic effect. However, β_1AR stimulation has a cell-wide response resulting in decreased APD and increased CaT amplitude. This specific control is lost when compartmentation is removed. Knowing which signaling components are affected by which receptors, and which cAMP pools and downstream effectors they control, is a critical first step to develop pharmaceutical compounds that act locally, thereby ensuring their specificity and avoiding arrhythmogenic side-effects.

We integrated the novel compartmental cAMP/PKA pathway with the CaMKII pathway present in the baseline model [28,40] via a physiological, population based approach. Soltis and Saucerman [45] recently described a computational model that includes both CaMKII and PKA pathways and identified a synergistic effect of these pathways on CaT amplitude. Consistent with their data, we find that βARS enhances CaMKII activity and phosphorylation of CaMKII substrates. This enhanced activity is due to enhanced Ca^{2+} cycling. In addition, we show that this effect is dose-dependent and more pronounced at fast rates. Enhanced CaMKII activity with increasing pacing rate (due to the accumulation of CaMKII activity) is larger than that due to βARS at a given rate, consistent with the concept that CaMKII is predominantly a frequency sensor [41]. Because βARS has important chronotropic effects in-vivo, a synergistic increase in CaMKII activity via both mechanisms is predicted. Experimental techniques for real-time monitoring of CaMKII activity in specific myocyte compartments are needed to fully characterize the βARS–CaMKII interactions and their mechanisms. Other interactions, such as those via cAMP-dependent activation of EPAC which has downstream effects on CaMKII, may be important. Recently, Mangmool et al. showed that this interaction is β1AR-specific and involves translocation of EPAC and CaMKII to the receptor complex via β-arrestin [49]. When more quantitative aspects of EPAC-dependent CaMKII activation become available, the compartmental model presented here will be able to include these localized and isoform specific interactions.

4.1. Comparison to existing models

Many simulation studies have included functional effects of βARS on cardiac electrophysiology (see Section 1.8 in the online data supplement for model comparisons). Most studies included only functional effects on substrates via a shift in parameters for a single pathway. Saucerman et al. [14] were the first to integrate a global model of the cAMP signaling cascade into a model of ventricular cell electrophysiology. Recently, these authors expanded their model [45] by combining the effects of CaMKII and cAMP/PKA on electrophysiological targets. Iancu et al. [11] were the first to develop a model which included localized aspects of cAMP signaling but not electrophysiological effects. These pioneering studies formed the basis for the model presented here, whose main novel characteristics include: (i) compartmental model of βARS and its effects on electrophysiology and CaT in canine ventricular myocyte; (ii) incorporation of both β_1AR and β_2AR isoforms to study physiological effects of compartmentation; (iii) a detailed population-based approach to integrate the cAMP/PKA and CaMKII pathways and their effects on a wide range of substrates.

4.2. Limitations

Due to the inherent complexity of the simulated system, the resulting model is complex and involves many parameters. This is because it is based on the actual mechanistic interactions between many proteins for both the signaling pathway and the electrophysiological model.

Parameter sensitivity analysis (online supplement section 1.6.1 and figs. S28-S30) provides insight into the contributions and relative importance of individual parameters. To facilitate application of this model, model code, including validation protocols, is available online in the Research Section of http://www.rudylab.wustl.edu. In addition, the model can be decomposed into two simpler modules (signaling and electrophysiology) that are connected through the phosphorylation levels. Thus, in investigations involving only electrophysiological measures, the phosphorylation levels can simply be fixed and only the electrophysiological module can be used. Similarly, other investigations may only require the signaling pathway.

Not all parameters are currently available from the experimental data. In addition, certain characteristics of the βAR signaling cascade are only available for rodents or are determined in biochemical reaction systems. However, major elements of the cascade (βAR density, AC activity, cAMP levels, I_{CaL} and I_{Ks} ISO concentration-dependence) and most electrophysiological properties of PKA substrates are available from canine ventricular myocytes. Nonetheless, a model based entirely on canine-specific experimental data is currently not feasible. Importantly, all parameters have a physiological interpretation and can in principle be determined experimentally. The parameter estimation procedure was designed such that parameters were determined from data reflecting direct steps in the βAR cascade whenever possible, in order to minimize uncertainties.

The exact effect of phosphorylation is still debated for some substrates, particularly the RyR [50]. Because the substrate data are based on whole-cell properties in the presence of maximal ISO stimulation, we do not distinguish between specific phosphorylation sites per substrate. For example, the I_{CaL} channel has multiple subunits with various PKA phosphorylation sites. The model reproduces the net effect on I_{CaL} of all phosphorylation sites combined. However, we do distinguish between the phosphorylation mechanisms (i.e., CaMKII versus PKA) using separate populations. Once electrophysiological and signaling data become available for individual phosphorylation sites, the population-based approach introduced here can be readily extended to incorporate this level of detail.

Long pacing sequences must be simulated to capture the phosphorylation time course, which means that it is computationally prohibitive to simulate microscopic Ca^{2+} events (e.g., Ca^{2+} sparks). As such, the model is limited to reproducing macroscopic Ca^{2+} properties. Similarly, the model employs a macroscopic, threshold-based SR store-overload induced Ca^{2+}-release mechanism.

Disclosures

None.

Acknowledgements

We thank Dr. Leonid Livshitz, Dr. Ali Nekouzadeh, Dr. Keith Decker, Namit Gaur, Tom O'Hara and Jiajing Xu, Washington University in St. Louis, and Daniel M. Johnson, Maastricht University, The Netherlands for helpful discussions.

This work was supported by the National Institutes of Health-National Heart, Lung, and Blood Institute (Grants R01-HL049054-18 and R01-HLR01033343-26) and Fondation Leducq Award to the Alliance for Calmodulin Kinase Signaling in Heart Disease (Grant 08CVD01) to Y. Rudy. This material is also based in part upon work supported by the National Science Foundation under Grant No. CBET-0929633 to Y. Rudy. Any opinions, findings and conclusions or recommendations expressed in this material are those of the authors and do not necessarily reflect the views of the National Science Foundation (NSF). Support by the Hein J.J. Wellens Foundation to J Heijman is acknowledged. P.G.A. Volders is supported by The Netherlands Heart Foundation (NHS 2007T51); and The Netherlands Organization for Scientific Research (Grant ZonMw Vidi 91710365). Y. Rudy is the Fred Saigh Distinguished Professor at Washington University in St. Louis and the Distinguished Hein J.J. Wellens Visiting Professor 2008–2009 at Maastricht University.

Appendix A. Supplementary data

Supplementary data to this article can be found online at doi:10.1016/j.yjmcc.2011.02.007.

References

[1] Rapundalo ST. Cardiac protein phosphorylation: functional and pathophysiological correlates. Cardiovasc Res 1998;38(3):559–88.
[2] Bers DM. Excitation–contraction coupling and cardiac contractile force. 2nd ed. Dordrecht ; London: Kluwer Academic; 2001.
[3] Scott JD, Pawson T. Cell signaling in space and time: where proteins come together and when they're apart. Science 2009;326(5957):1220–4.
[4] Kang M, Chung KY, Walker JW. G-protein coupled receptor signaling in myocardium: not for the faint of heart. Physiology 2007;22:174–84.
[5] Steinberg SF, Brunton LL. Compartmentation of G protein-coupled signaling pathways in cardiac myocytes. Annu Rev Pharmacol Toxicol 2001;41:751–73.
[6] Vandecasteele G, Rochais F, Abi-Gerges A, Fischmeister R. Functional localization of cAMP signalling in cardiac myocytes. Biochem Soc Trans 2006;34(Pt 4):484–8.
[7] Mauban JRH, O'Donnell M, Warrier S, Manni S, Bond M. AKAP-scaffolding proteins and regulation of cardiac physiology. Physiology 2009;24:78–87.
[8] Nikolaev VO, Moshkov A, Lyon AR, Miragoli M, Novak P, Paur H, et al. β2-adrenergic receptor redistribution in heart failure changes cAMP compartmentation. Science 2010;327(5973):1653–7.
[9] Grimm M, Brown JH. β-Adrenergic receptor signaling in the heart: role of CaMKII. J Mol Cell Cardiol 2010;48(2):322–30.
[10] Rudy Y, Silva JR. Computational biology in the study of cardiac ion channels and cell electrophysiology. Q Rev Biophys 2006;39(1):57–116.
[11] Iancu RV, Ramamurthy G, Warrier S, Nikolaev VO, Lohse MJ, Jones SW, et al. Cytoplasmic cAMP concentrations in intact cardiac myocytes. Am J Physiol Cell Physiol 2008;295(2):C414–22.
[12] Violin JD, DiPilato LM, Yildirim N, Elston TC, Zhang J, Lefkowitz RJ. β2-adrenergic receptor signaling and desensitization elucidated by quantitative modeling of real time cAMP dynamics. J Biol Chem 2008;283(5):2949–61.
[13] Xin W, Tran TM, Richter W, Clark RB, Rich TC. Roles of GRK and PDE4 activities in the regulation of β2 adrenergic signaling. J Gen Physiol 2008;131(4):349–64.
[14] Saucerman JJ, Brunton LL, Michailova AP, McCulloch AD. Modeling β-adrenergic control of cardiac myocyte contractility in silico. J Biol Chem 2003;278(48):47997–8003.
[15] Zeng J, Rudy Y. Early afterdepolarizations in cardiac myocytes: mechanism and rate dependence. Biophys J 1995;68(3):949–64.
[16] Faber GM, Rudy Y. Calsequestrin mutation and catecholaminergic polymorphic ventricular tachycardia: a simulation study of cellular mechanism. Cardiovasc Res 2007;75(1):79–88.
[17] Kuzumoto M, Takeuchi A, Nakai H, Oka C, Noma A, Matsuoka S. Simulation analysis of intracellular Na+ and Cl− homeostasis during β1-adrenergic stimulation of cardiac myocyte. Prog Biophys Mol Biol 2008;96(1–3):171–86.
[18] Iyer V, Hajjar RJ, Armoundas AA. Mechanisms of abnormal calcium homeostasis in mutations responsible for catecholaminergic polymorphic ventricular tachycardia. Circ Res 2007;100(2):e22–31.
[19] Warrier S, Ramamurthy G, Eckert RL, Nikolaev VO, Lohse MJ, Harvey RD. cAMP microdomains and L-type Ca2+ channel regulation in guinea-pig ventricular myocytes. J Physiol 2007;580(Pt3):765–76.
[20] Leroy J, Abi-Gerges A, Nikolaev VO, Richter W, Lechêne P, Mazet J-L, et al. Spatiotemporal dynamics of β-adrenergic cAMP signals and L-type Ca2+ channel regulation in adult rat ventricular myocytes: role of phosphodiesterases. Circ Res 2008;102(9):1091–100.
[21] Madamanchi A. β-Adrenergic receptor signaling in cardiac function and heart failure. Mcgill J Med 2007;10(2):99–104.
[22] Nikolaev VO, Bunemann M, Schmitteckert E, Lohse MJ, Engelhardt S. Cyclic AMP imaging in adult cardiac myocytes reveals far-reaching β1-adrenergic but locally confined β2-adrenergic receptor-mediated signaling. Circ Res 2006;99(10):1084–91.
[23] Calaghan S, Kozera L, White E. Compartmentalisation of cAMP-dependent signalling by caveolae in the adult cardiac myocyte. J Mol Cell Cardiol 2008;45(1):88–92.
[24] He JQ, Balijepalli RC, Haworth RA, Kamp TJ. Crosstalk of β-adrenergic receptor subtypes through Gi blunts beta-adrenergic stimulation of L-type Ca2+ channels in canine heart failure. Circ Res 2005;97(6):566–73.
[25] Nagykaldi Z, Kem D, Lazzara R, Szabo B. Canine ventricular myocyte β2-adrenoceptors are not functionally coupled to L-type calcium current. J Cardiovasc Electrophysiol 1999;10(9):1240–51.
[26] Altschuld RA, Starling RC, Hamlin RL, Billman GE, Hensley J, Castillo L, et al. Response of failing canine and human heart cells to β2-adrenergic stimulation. Circulation 1995;92(6):1612–8.
[27] Rozec B, Gauthier C. β3-adrenoceptors in the cardiovascular system: putative roles in human pathologies. Pharmacol Ther 2006;111(3):652–73.

[28] Decker KF, Heijman J, Silva JR, Hund TJ, Rudy Y. Properties and ionic mechanisms of action potential adaptation, restitution, and accommodation in canine epicardium. Am J Physiol Heart Circ Physiol 2009;296(4):H1017–26.
[29] Hund TJ, Decker KF, Kanter E, Mohler PJ, Boyden PA, Schuessler RB, et al. Role of activated CaMKII in abnormal calcium homeostasis and INa remodeling after myocardial infarction: insights from mathematical modeling. J Mol Cell Cardiol 2008;45(3):420–8.
[30] Volders PG, Stengl M, van Opstal JM, Gerlach U, Spatjens RL, Beekman JD, et al. Probing the contribution of IKs to canine ventricular repolarization: key role for β-adrenergic receptor stimulation. Circulation 2003;107(21): 2753–60.
[31] Rocchetti M, Besana A, Gurrola GB, Possani LD, Zaza A. Rate dependency of delayed rectifier currents during the guinea-pig ventricular action potential. J Physiol 2001;534(Pt 3):721–32.
[32] Silva J, Rudy Y. Subunit interaction determines IKs participation in cardiac repolarization and repolarization reserve. Circulation 2005;112(10):1384–91.
[33] Rocchetti M, Freli V, Perego V, Altomare C, Mostacciuolo G, Zaza A. Rate dependency of β-adrenergic modulation of repolarizing currents in the guinea-pig ventricle. J Physiol 2006;574(Pt 1):183–93.
[34] Severi S, Corsi C, Rocchetti M, Zaza A. Mechanisms of beta-adrenergic modulation of I(Ks) in the guinea-pig ventricle: insights from experimental and model-based analysis. Biophys J 2009;96(9):3862–72.
[35] Volders PG, Kulcsár A, Vos MA, Sipido KR, Wellens HJ, Lazzara R, et al. Similarities between early and delayed afterdepolarizations induced by isoproterenol in canine ventricular myocytes. Cardiovasc Res 1997;34(2): 348–59.
[36] Curran J, Hinton MJ, Ríos E, Bers DM, Shannon TR. β-adrenergic enhancement of sarcoplasmic reticulum calcium leak in cardiac myocytes is mediated by calcium/calmodulin-dependent protein kinase. Circ Res 2007;100(3):391–8.
[37] Despa S, Tucker AL, Bers DM. Phospholemman-mediated activation of Na/K-ATPase limits [Na]i and inotropic state during β-adrenergic stimulation in mouse ventricular myocytes. Circulation 2008;117(14):1849–55.
[38] Sridhar A, da Cunha DN, Lacombe VA, Zhou Q, Fox JJ, Hamlin RL, et al. The plateau outward current in canine ventricle, sensitive to 4-aminopyridine, is a constitutive contributor to ventricular repolarization. Br J Pharmacol 2007;152(6):870–9.
[39] Banyasz T, Horvath B, Virag L, Barandi L, Szentandrassy N, Harmati G, et al. Reverse rate dependency is an intrinsic property of canine cardiac preparations. Cardiovasc Res 2009;84(2):237–44.
[40] Livshitz LM, Rudy Y. Regulation of Ca2+ and electrical alternans in cardiac myocytes: role of CAMKII and repolarizing currents. Am J Physiol Heart Circ Physiol 2007;292(6):H2854–66.
[41] De Koninck P, Schulman H. Sensitivity of CaM kinase II to the frequency of Ca2+ oscillations. Science 1998;279(5348):227–30.
[42] Huke S, Bers DM. Temporal dissociation of frequency-dependent acceleration of relaxation and protein phosphorylation by CaMKII. J Mol Cell Cardiol 2007;42(3):590–9.
[43] Hagemann D, Kuschel M, Kuramochi T, Zhu W, Cheng H, Xiao RP. Frequency-encoding Thr17 phospholamban phosphorylation is independent of Ser16 phosphorylation in cardiac myocytes. J Biol Chem 2000;275(29):22532–6.
[44] Priori SG, Corr PB. Mechanisms underlying early and delayed afterdepolarizations induced by catecholamines. Am J Physiol 1990;258(6 Pt 2):H1796–805.
[45] Soltis AR, Saucerman JJ. Synergy between CaMKII substrates and beta-adrenergic signaling in regulation of cardiac myocyte Ca(2+) handling. Biophys J 2010;99 (7):2038–47.
[46] Kashimura T, Briston SJ, Trafford AW, Napolitano C, Priori SG, Eisner DA, et al. In the RyR2(R4496C) mouse model of CPVT, beta-adrenergic stimulation induces Ca waves by increasing SR Ca content and not by decreasing the threshold for Ca waves. Circ Res 2010;107(12):1483–9.
[47] Rochais F, Vandecasteele G, Lefebvre F, Lugnier C, Lum H, Mazet J-L, et al. Negative feedback exerted by cAMP-dependent protein kinase and cAMP phosphodiesterase on subsarcolemmal cAMP signals in intact cardiac myocytes: an in vivo study using adenovirus-mediated expression of CNG channels. J Biol Chem 2004;279 (50):52095–105.
[48] Murray AJ. Pharmacological PKA inhibition: all may not be what it seems. Sci Signal 2008;1(22):re4.
[49] Mangmool S, Shukla AK, Rockman HA. Beta-arrestin-dependent activation of Ca(2+)/calmodulin kinase II after beta(1)-adrenergic receptor stimulation. J Cell Biol 2010;189(3):573–87.
[50] Bridge JHB, Savio-Galimberti E. What are the consequences of phosphorylation and hyperphosphorylation of ryanodine receptors in normal and failing heart? Circ Res 2008;102(9):995–7.